Energy Conversion and Management 225 (2020) 113444

Contents lists available at ScienceDirect

Energy Conversion and Management

journal homepage: www.elsevier.com/locate/enconman

Energetic analysis and optimal design of a CHP plant in a frozen food processing factory through a dynamical simulation model

Filippo Catalano [a], Claudio Perone [b,*], Valentino Iannacci [c], Alessandro Leone [d], Antonia Tamborrino [d], Biagio Bianchi [d]

[a] Department of Biosciences and Territory, University of Molise, C.da Fonte Lappone, Pesche, IS, Italy
[b] Department of the Science of Agriculture, Food and Environment, University of Foggia, Via Napoli, 25, Foggia 71122, Italy
[c] Fruttagel S.C.P.A, Via Statale Sannitica, 87 - Piane di Larino, Larino, CB, Italy
[d] Department of Agricultural and Environmental Science, University of Bari Aldo Moro, Via Amendola 165/A, Bari, Italy

ARTICLE INFO

Keywords:
Cogeneration
Dynamical Simulation
Multi-objective analysis optimization
Food Industry
Exergy analysis

ABSTRACT

The proper design of cogeneration plants requires the choice of the technologies that best fits the ratio between heating and power loads. In this paper, a dynamical procedure of selecting and dimensioning a cogeneration plant, using deep and detailed energy, exergy and economic analysis of the entire production process of a frozen food production factory is proposed. The results highlight that a design method, based on a dynamic simulation, optimizes the energy efficiency of the food processing plant involved in the experimental test. Indeed, by considering the overall efficiency of the CHP + National grid system, the energy efficiency is 6% higher in the case of dynamic compared to a static design, resulting in better overall use of resources with a possible lower level of environmental impact. Moreover, the CHP plant designed with the proposed method generates electrical energy which appropriately matches that required by the process, with a surplus/deficit less than 4%, while the classic method never covers the amount required and results in a deficit greater than 20%. Finally, the annual savings of the solution derived from the dynamic method is 12% higher than that obtained with a traditional design technique. Considering the greater absolute cost of the cogeneration plant, this dynamic approach results in more profitable annual investment margins for the company.

1. Introduction

Cogeneration arises from an attempt to recover in a useful way all or part of the heat that must necessarily be discharged from a thermal engine or power station. The heat recovered could be effectively used in industry, construction or district heating. It is well known that primary energy savings, compared to the separate generation of heat and electricity, is relevant due to a better exploitation of fuel/resources [1]. From the technologies available today, it is also possible to choose the one that best fits the ratio between the required heat and power [2].

In particular, some types of machines used in cogeneration, such as micro gas turbines (MGTs), allow the modulation of power production as a function of the variability of user demand without incurring significant loss of performance [3]. This should lead to well-designed and planned production processes with cogeneration plants, with clear energy and exergetic savings since the greater the demand for energy, the more the industry is interested in using this type of plant [2,4-6].

Many methods have been studied to reduce greenhouse gas emissions, in particular, the introduction of cogeneration systems for industrial plants [7,8] and civil use [9,10]. This results in a significant reduction in the production of CO_2 emission [11-13]. All this is greatly stimulated from an energetic point of view thanks to the reduction and recovery of waste heat [14], and from an economic point of view thanks to a reduction in energy costs [15]. These systems are more sustainable if the energy carrier employed is produced from waste processing in the same industry or from other neighboring industries or farms, such as, for example, food industries [17-22].

Regarding the heat loss in current energy systems, it is estimated that it is high enough in approximately 30% [23] of power-only generation plants, therefore, this leads to the possibility of obtaining strong energy recovery and/or savings. The state of the art of technologies used in modern cogeneration plants achieves efficiencies of 90% (fuel input converted to useful energy), while the global average for traditional

* Corresponding author.
E-mail addresses: f.catalano1@studenti.unimol.it (F. Catalano), claudioperone@gmail.com, c.perone1@studenti.unimol.it (C. Perone), alessandro.leone@uniba.it (A. Leone), antonia.tamborrino@uniba.it (A. Tamborrino), biagio.bianchi@uniba.it (B. Bianchi).

https://doi.org/10.1016/j.enconman.2020.113444
Received 27 May 2020; Received in revised form 10 September 2020; Accepted 11 September 2020

Nomenclature

A	Heat exchanger surface (m^2)
e	specific (mass) exergy (J/kg)
$\dot{E}$	Required Power (W)
$\dot{Ex}$	Total Exergy Flux (W)
h	Specific enthalpy (J/kg)
H	Total enthalpy (J)
$\dot{m}$	Mass flow rate (kg/s)
$\dot{n}$	Molar flow rate (mol/s)
N	Number of Micro Turbines
NTU	Number of Thermal Units (-)
p	Pressure (bar)
$\dot{Q}$	Thermal Power (W)
r	partialization (-)
R_0	Universal Gas Constant (J/mol K)
s	Specific entropy (J/kg K)
U	Heat exchanger transfer coefficient (W/m^2 K)
$\dot{W}$	Mechanical/Electric power (W)

Greek

α	air–fuel mass ratio (-)
ϵ	specific (molar) exergy (J/mol)
η	efficiency (-)

Subscript

0	dead state
1	exhaust gas after combustion, hot water after pre-heating
2	superheated steam, exhaust gas after expansion
3	exhaust gas after afterburning
A	air
B	Boiler
C	Combustion
CH_4	Natural gas
CMP	CoMPressor
e	electrical
EG	Exhaust gases
f	formation (enthalpy)
h	heat
ICE	Internal Combustion Engine
in	inlet
L	cooLant
LHV	Lower Heating Value
m	mix
max	maximum
MGT	Micro Gas Turbine
oth	other gases
O_2	Oxygen
out	outlet
SHS	Super Heated Steam
th	thermal
w	water

Superscript

(k)	k-th Boiler
¯	mean value

power generation plants based on fossil fuels is 35–37% [23].

However, the literature reviews cited above lead to a common result. Despite the numerous papers related to cogeneration plant design in industrial and civil applications, there are not many examples regarding the use of combined heat and power (CHP) plants in the agricultural and food industry chain, especially those where a high load variability often occurs

About 20 years ago, Fantozzi et al. [24] focused their attention on an Italian pasta and animal feed factory, determining the type and scale of the possible internal combustion engines (ICEs) and gas turbine (GT) for system configuration, which was evaluated only on the basis of monthly energy consumption. More recently, some authors have paid particular attention to economic and environmental feasibility of CHP plants in the food industry. Freschi et al. [25] analyzed both the economic gains and environmental aspects at the same time by means of a dynamic simulation tool applied to the food industry. However, as an energy indicator they used only the Primary Energy Saving coefficient (PES), one of the three parameters proposed in this paper, which was applied both to CHP plants and trigeneration systems. Optimization was carried out using mixed-integer linear programming.

These studies highlight that the food industry is well suited to the use of cogeneration, whose design is today primarily based on an energy and economic analysis of the process as a whole, comparing results before and after the installation of a cogeneration plant. Some reviews can be found in [2,3,26].

Generally, in the literature research can be found regarding energetic [1,16,27,28], economic [29,30] and exergetic [31,32] aspects concerning CHP plants, but only a few authors provide a complete analysis of these three aspects as a whole for the food industry [33]. Studies are frequently carried out separately from many CHP applications, which however provide important indicators that can be used as useful support for the optimum selection and sizing of a cogeneration plant as applied to the food industry [34,35]. In particular, Zisopoulos et al. [34] developed a careful review of the different applications of these indicators, which were used separately or, at most, in pairs.

Only in recent studies multi-objective analysis of CHP plants was carried out in order to find the optimum configuration of the plant [36] and the optimization of plant operation [37], but never for applications of the food industry with high load variability. In fact, in most food industries the energy requirements produce an unpredictable trend due to the high variability of raw materials during an entire year. This increases the difficulty in optimizing the entire production process and in particular energy management. In any case, multi-objective analysis is considered to be a powerful tool for determining the best trade-off solutions among conflicting objectives [38]. The choice of suitable objective functions is not a simple task. Generally, an optimization of economic parameters leads to a worsening in energy parameters, and vice versa. For this reason, in many cases the analysis is not carried out by using dynamical simulation, although an exception may be made for some applications, mainly regarding civil engineering [2,39].

Due to the previously cited high variability of energy loads, a cogeneration plant may have serious difficulty in following heat tracking or power tracking. Under these conditions, CHP plant operation, whose design is traditionally based on only monthly consumption of electricity and natural gas as well as on installed power and the number of working hours (static analysis), may function in an unpredictable and inefficient way. This confirms the need for the dynamic analysis described below, which is carried out on an hourly basis of energy flows and combined with multi-objective optimization techniques in order to determine the right configuration and type of CHP plant as well as its correct size.

In this study, an energy analysis of the frozen food industry was carried out according to well-known and consolidated techniques. Then, a dynamical procedure was proposed to simulate, select and size a cogeneration plant through an energy-exergy analysis of the heat and power generation process and a simplified economic analysis, by using a multi-objective optimization procedure.

2. Materials and methods

2.1. Processing facilities

The energy analysis and successive simulation–optimization steps were carried out in an Italian cooperative firm that processes and markets canned and frozen foods, Fruttagel S.C.P.A., consisting in a main plant in Alfonsine (Ravenna), Italy, and a second factory in Larino (Campobasso), Italy. In particular, this paper refers to the plant located in Larino, which includes all the activities of pre-processing and storage of frozen products. The plant, which is the focus of this study, has three separate production lines of frozen foods:

- leaf vegetables: spinach, chard and others;
- grilled vegetables: eggplant, zucchini and peppers;
- vegetable soup: different types of frozen vegetables, cut into slices and cubes of various size, stored in bins, then mixed and packaged at the plant in Alfonsine.

The facility consists of:

- an area with processing lines and freezing facilities at −40 °C ;
- cold rooms for storage of raw materials (one cold room at 0–4 °C for finished products, and two cold rooms at −40 °C);
- laboratory and offices;
- technical installations for the production processes.

Due to the high variability of processed foods, the production trend is highly seasonal as it is strongly influenced by the fresh product harvesting seasons. This makes it impossible to determine a typical month. Moreover, as also highlighted below, it is not possible to define a typical week or even more so, a typical day, because of the short-term unpredictability of agricultural production.

2.2. Energy supply and consumption

Typically, many food industries have a high heat demand for processing raw materials as well as for electric energy to run all the process machinery [5].

The main energy sources used by the company studied are:

- electric power for the cooling station, the laboratory, offices and auxiliary services (lights, air compressors, water pumps, etc.),
- natural gas to feed the boilers,
- natural gas for grilled vegetables production (not included in this analysis).

To meet the need for electricity, the company is connected at Medium Voltage (MV) to the national grid. In particular, Table 1 shows the total installed power, taking into account each factory division (including the freezing plant), the refrigeration units for storage for raw materials and finished products, the compressed air unit, and auxiliary systems and offices. It can be noted that the processing lines have a higher installed power, as expected. This is mainly due to the numerous operations that take place within each line, such as the separation of impurities from the raw materials, the selection, the washing and freezing of the products as well as the transport of materials (products, by-products and waste material) from one machine to another. The processing plant is also equipped with a control unit for the production of compressed air, consisting in 3 compressors of about 7.5 kW each.

Table 1
Electric power installation for different uses.

Description of the user	Power[kW]
Processing lines and freezing plants (-40 °C)	810
Storage of raw materials (0 – 4 °C)	160
Storage of raw finished products: cold room 1 (-40 °C)	115
Storage of raw finished products: cold room 2 (-40 °C)	250
Compressed air unit	22.5
Auxiliary system and offices	110.5

A large amount of power is also required for the refrigeration of raw and finished products, while a lower request comes from pneumatic machines and offices (lighting, equipment and air conditioning).

Regarding the heating loads, the heating plant consists of two boilers, one 3.5 MW and the other 4.5 MW, for the production of superheated steam at 190 °C and 10 bar. The cooling station has a total installed power of 1.3 MW, and consists of 6 vapor compression chillers with ammonia as the refrigerant.

In addition to detecting monthly trends of power and heat for the company, direct measurements of electric power absorbed $\dot{W}$ and heat output required $\dot{Q}_{SHS}(t)$ for the production of superheated steam were made. Electricity and gas consumption data were acquired hourly for one year. Regarding the hourly heat output $\dot{Q}_{SHS}(t)$, this was calculated using time trends of the incoming and outgoing hot fluid temperature $T_{in}(t)$ and $T_{out}^{(k)}(t)$ (k ∈ {1, 2}), pressure $p^{(k)}(t)$, entropy $s^{(k)}(t)$ and average flow rate $\dot{m}^{(k)}(t)$ for each *k-th* boiler, then adding up the individual heat $\dot{Q}_k(t)$ [40]:

$$\dot{Q}^{(k)} = \dot{m}^{(k)}\left[h_w\left(T_{out}^{(k)}, p_{out}^{(k)}\right) - h_w(T_{in}, p_{in})\right]; k \in \{1,2\} \quad (1)$$

$$\dot{Q}_{SHS} = \sum_{k=1}^{2}\dot{Q}^{(k)} \quad (2)$$

where $k = 1$ refers to the nominal power boiler 4.5 MW, and $k = 2$ refers to the nominal power boiler 3.5 MW, while h_w is the enthalpy of water at a given temperature and pressure.

This represents the first step of our procedure, which was finalized to calculate all the input data for the following dynamic analysis of the simulated cogeneration plants.

2.3. CHP tested configurations

In Table 2 we show a list of available technologies used in CHP plants, and below their different uses for industrial applications are explain in detail [41,42].

About the internal combustion engines not equipped with a pressurized jacket it is worth remembering that about half of the obtained heat is available at temperatures below 100 °C and the other at temperatures around 350–450 °C. Therefore, it is necessary to continuously evaluate what type of load tracking method (heat or power) is

Table 2
Available CHP technologies and their main use.

CHP	
Engines with/without pressurized jacket	Combustion engine CHP plants can handle wide load range in combination with the high efficiency at different loads and the fast starts and stops. The pressurized jacket allows obtaining heat at higher temperature if required.
Large Gas Turbines	Large Gas Turbines CHP plants (power of at least 1 MW) are most suitable for high and stable heat and power loads due to their quite slow starts and stops
Microturbines with/without afterburner	Microturbines produce thermal energy only at high temperature. Microturbines, while being characterized by a generally lower yield than that of large gas turbines, often become better performing when partialized.
Combined plants (Gas + Steam Turbines)	Steam turbine CHP plants are most widely used in the industrial sector where high quantity and high-quality heat is required. In general, these plants will be designed around the heat demand with electricity as the secondary product

convenient to use to lose as little energy as possible.

Regarding large gas turbines, they are not suitable when frequent shutdowns occur due to variability in product demand: it is necessary to avoid frequent intermittent operation for a correct and efficient use of gas turbines. In fact, due to the very high temperatures reached by the early stages of blade system, high mechanical stress occurs during the fast heating and cooling periods.

On the other hand, particularly interesting is the solution involving the use of micro gas turbines, generally made of ceramic material, showing relatively low working temperature (below 900 ÷ 950 °C) making it possible to gradually turn them off and on, according to appropriate programming.

Furthermore, the flexibility of microturbines allows partializing the total electric power of the cogeneration plant without having an excessive reduction of the efficiency. In fact, it is possible turning on at nominal power only those microturbines which provide to get as close as possible to the heat or electric power demand.

Finally, combined cycle power plants are mostly used when high and stable heat load is required compared to less important electricity requirement.

Sometimes an afterburner is added to the solution with gas microturbines and a backup boiler to the solution with engines. In this way, the sizing of the CHP modules can be based on a fraction of the maximum heat demand avoiding, so, moments of surplus of electricity that do not justify the cost effectiveness.

Therefore, due to the high demand and variability of both electricity and heat of the studied application, it is possible to assess the most suitable configurations of a medium size cogeneration plant using the following machines:

- pressurized internal combustion engines (ICEs),
- micro-gas turbines assembled in cluster (MGTs).

Two configurations have been considered. The first involves internal combustion engines (in a cluster of a suitable number N) with a backup boiler (Fig. 1), while microturbines (in a cluster of a suitable number N) equipped with an afterburner (Fig. 2) constitute the second configuration.

The engines used in the first configuration (Fig. 1) are equipped with a jacket and an intermediate fluid as coolant flowing in it, which is able to recover part of the waste heat at low temperature. Process water is preheated in a counter-current low temperature heat exchanger while the cooling fluid is recycled in the jacket. Steam is generated from the preheated water by using the exhausted gases in a high temperature heat exchanger. If necessary, a backup boiler could be used to cover any additional steam request.

In the second solution (Fig. 2) the air is compressed in each microturbine group then mixed with the natural gas, burned and finally expanded in the gas turbine. If necessary, the temperature of the exhausted gases is raised in an afterburner to meet the required heating load. Steam is then generated in a counter-current heat exchanger.

Plant configurations can be completed with the integration in the micro-grid of the photovoltaic system. In order to maximize the benefits arising from the use of CHP, the study was carried out through dynamic simulation taking into account energy, exergy and economic aspects. The simulations were performed for each one configuration shown in Table 3, by determining the operating parameters of each machine on an hourly base.

When the CHP solution is integrated with a photovoltaic system, it mainly produces the electricity necessary for the cold rooms. This is particularly useful when the production lines are turned off, resulting in a lack of heat load. Overnight electricity can be purchased from the grid at a more favorable tariff. This avoids the CHP working as a simple power generator, which would lead to the production of waste heat with a high environmental impact.

Finally, it is important to note that the existing refrigeration system still provides the cooling load, so the proposed solutions are CHP plants and not CCHP (Combined Cooling, Heating and Power) plants. In fact, in trigeneration systems, where cooling load is supplied by using an absorption chiller, the performance of cooling power can be, in some cases, lower than that of compression chillers [23,43].

2.4. Numerical modelling

As for the solution with an engine, the schematic representation of the plant is shown in Fig. 1 and the main mass, energy and exergy time-

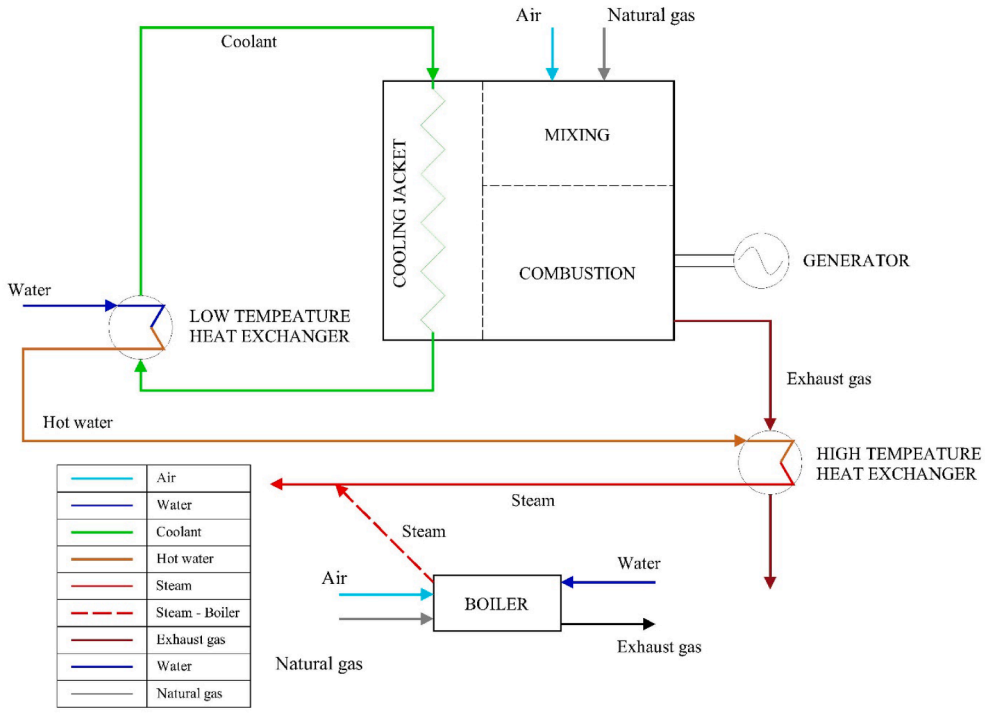

Fig. 1. Schematic representation of simulated plant with engines as CHP.

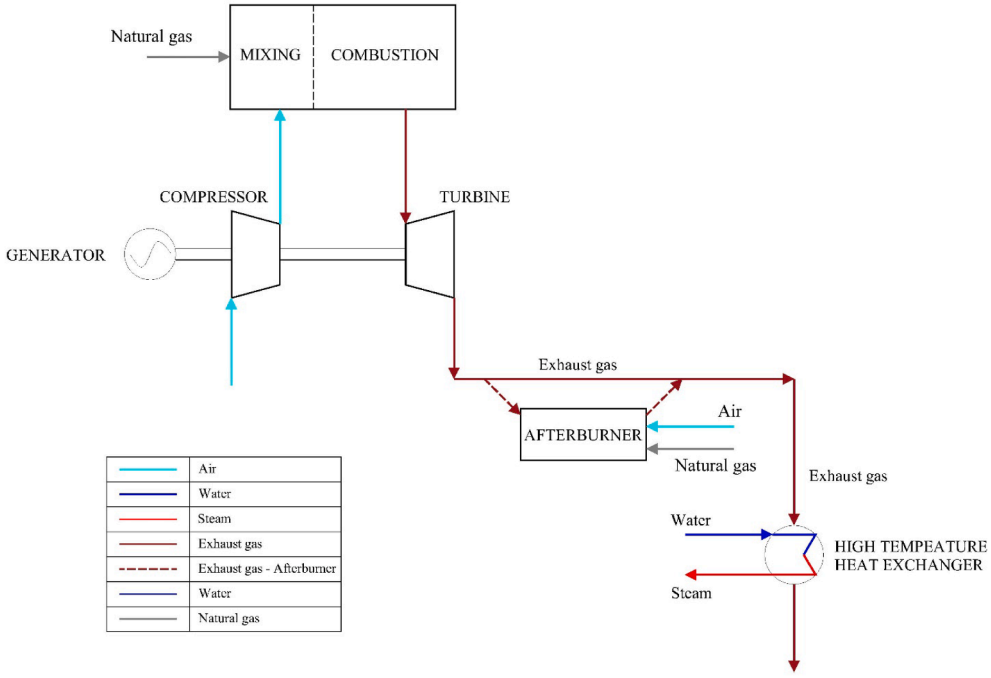

Fig. 2. Schematic representation of simulated plant with microturbines as CHP.

Table 3
Simulated plant configurations.

CHP	Renewables	Load tracking
Engines with backup boiler	Photovoltaic (Yes/No)	Heat
Engines with backup boiler	Photovoltaic (Yes/No)	Power
Microturbines with afterburner	Photovoltaic (Yes/No)	Heat
Microturbines with afterburner	Photovoltaic (Yes/No)	Power

varying balance equations are listed below.

Mixing (other gases ≈ N_2):

Mixing of gases, air (A), composed mainly of Oxygen (O_2) and other gases, and natural gas (CH_4), concerns only mass (molar) and the exergy balance equations since energy does not vary during the mixing process. In the equation 3, the sum of molar fluxes of O_2 ($\dot{n}_{O_2}$), of CH_4 ($\dot{n}_{CH_4}$) and of the other gases ($\dot{n}_{oth}$) matches the molar flux of the mixture ($\dot{n}_m$):

$$\dot{n}_m = \dot{n}_A + \dot{n}_{CH_4} = \dot{n}_{oth} + \dot{n}_{O_2} + \dot{n}_{CH_4} \quad (3)$$

The same occurs for the exergy (ε_{O_2} is the specific molar exergy of O_2, ε_{CH_4} is the specific molar exergy of CH_4, and ε_{oth} is the specific molar exergy of the other gases) before the irreversible mixing occurs ($\varepsilon_{m,in}$):

$$\dot{n}_m \varepsilon_{m,in} = \dot{n}_{oth}\varepsilon_{oth} + \dot{n}_{O_2}\varepsilon_{O_2} + \dot{n}_{CH_4}\varepsilon_{CH_4} \quad (4)$$

and after irreversible mixing ($\varepsilon_{m,out}$) [44]:

$$\dot{n}_m \varepsilon_{m,out} = \dot{n}_{oth}\left[\varepsilon_{oth} + R_0 T_0 ln\left(\frac{\dot{n}_{oth}}{\dot{n}_m}\right)\right] + \dot{n}_{O_2}\left[\varepsilon_{O_2} + R_0 T_0 ln\left(\frac{\dot{n}_{O_2}}{\dot{n}_m}\right)\right] + \dot{n}_{CH_4}\left[\varepsilon_{CH_4} + R_0 T_0 ln\left(\frac{\dot{n}_{CH_4}}{\dot{n}_m}\right)\right] \quad (5)$$

where R_0 is the Universal Gas Constant, and T_0 is the dead state temperature. The total exergy flux can be calculated as the difference between input ($\varepsilon_{m,in}$) and output ($\varepsilon_{m,out}$) exergy fluxes:

$$\dot{E}x_m = \dot{n}_m\left(\varepsilon_{m,in} - \varepsilon_{m,out}\right) = -\dot{n}_{other}R_0T_0 ln\left(\frac{\dot{n}_{oth}}{\dot{n}_m}\right) - \dot{n}_{O_2}R_0T_0 ln(x_{O_2}) - \dot{n}_{CH_4}R_0T_0 ln(x_{CH_4}) \quad (6)$$

Combustion:

Regarding combustion, the mass balance equals the mass flow rate of the mixture ($\dot{m}_m$) with that of the exhaust gases ($\dot{m}_{EG}$), where the latter is the sum of air and methane flow rate, and α_m is the air–fuel mass ratio (depending on the corresponding molar flow rates):

$$\dot{m}_{EG} = \dot{m}_m = (1+\alpha_m)\dot{m}_{CH_4} \quad (7)$$

Energy balance requires further steps. The Lower Heating Value of methane H_{LHV,CH_4} is converted into heat ($\dot{Q}_C$), using the standard enthalpies of formation of the individual compounds of the combustion reaction (h_{f,CH_4}, h_{f,O_2}, h_{f,CO_2}, h_{f,H_2O}):

$$\dot{Q}_C = \dot{m}_{CH_4}\left[h_{f,CH_4} + 2h_{f,O_2} - \left(h_{f,CO_2} + 2h_{f,H_2O}\right)\right] = \dot{m}_{CH_4}H_{LHV,CH_4} \quad (8)$$

and into power:

$$\dot{W} = r\dot{W}_{max} = \left[\eta_{eICE}\left(r, \dot{W}_{max}\right)\right]\dot{Q}_C \quad (9)$$

where η_{eICE} is the electrical efficiency of the Internal Combustion Engine (ICE) depending on its partialization (r) and, possibly on the maximum electrical power ($\dot{W}_{max}$) of the ICE.

The enthalpy of the exhaust gases after combustion is calculated by summing to the initial enthalpy of the mixture and the heat generated, either not converted into electrical power or transferred to the coolant or dispersed into the environment (the last quantity is taken into account using the thermal efficiency η_{thICE} of the ICE):

$$h_{EG}(T_{EG1}) = \alpha_M h_A(T_0) + h_{CH_4}(T_0) + \frac{\eta_{thICE}\left(r, \dot{W}_{max}\right)\varepsilon_{thm}H_{LHV,CH_4}}{(1+\alpha_M)} \quad (10)$$

The exergy of the exhaust gases is calculated by using standard formulations [44], that takes into account enthalpy h and entropy s of individual compounds both depending on temperature (T_{EG1} and T_0 respectively) and pressure p_0:

$\dot{n}_{EG}\varepsilon_{EG1}$

$$= \dot{n}_{oth}\left\{\varepsilon_{oth} + R_0 T_0 ln\left(\frac{\dot{n}_{oth}}{\dot{n}_m}\right) + [h_{oth}(T_{EG1}, p_0) - h_{oth}(T_0, p_0)] + T_0[s_{oth}(T_{EG1}, p_0) - s_{oth}(T_0, p_0)]\right\} + \dot{n}_{O_2}\left\{\varepsilon_{O_2} + R_0 T_0 ln\left(\frac{\dot{n}_{O_2}}{\dot{n}_m}\right) + [h_{O_2}(T_{EG1}, p_0) - h_{O_2}(T_0, p_0)] + T_0[s_{O_2}(T_{EG1}, p_0) - s_{O_2}(T_0, p_0)]\right\} + \dot{n}_{CH_4}\left\{\varepsilon_{CH_4} + R_0 T_0 ln\left(\frac{\dot{n}_{CH_4}}{\dot{n}_m}\right) + [h_{CH_4}(T_{EG1}, p_0) - h_{CH_4}(T_0)] + T_0[s_{CH_4}(T_{EG1}, p_0) - s_{CH_4}(T_0)]\right\} \quad (11)$$

Again the total exergy flux is calculated by the difference between input ($\dot{m}_{EG} e_{m,out}$) and output ($\dot{m}_{EG} e_{EG1}$):

$$\dot{E}x_c = \dot{n}_{EG}\varepsilon_{m,out} - \dot{n}_{EG}\varepsilon_{EG1} = \dot{m}_{EG} e_{m,out} - \dot{m}_{EG} e_{EG1} \quad (12)$$

Engine refrigerator:

Using the same procedure adopted to calculate the enthalpy of the exhausted gases, the total heat $\dot{Q}_L$ transferred to the coolant is easily obtained:

$$\dot{Q}_L = \dot{m}_L c_L (T_{L1} - T_{L0}) = \left[1 - \eta_{eICE}\left(r, \dot{W}_{max}\right) - \eta_{thICE}\left(r, \dot{W}_{max}\right)\right] \frac{r\dot{W}_{max}}{\eta_{eICE}\left(r, \dot{W}_{max}\right)} \quad (13)$$

From the last equation the output temperature of the coolant T_{L1} is also easily calculated. Exergy flux is computed using standard formulation [44]:

$$\dot{E}x_L = -\dot{Q}_L\left(\frac{1}{T_L} - \frac{1}{T_c}\right) \quad (14)$$

Water-Coolant heat exchanger:

In this case, the standard formulation for a counter current heat exchanger is used: where U_{LW} and A_{LW} are the heat exchange global coefficient and the total area of the heat exchanger respectively, η_{LW} is the exchanger efficiency, ω_{LW} is the heat capacity ratio, NTU_{LW} is the Number of Thermal Units. Water is heated by raising its temperature from T_{w0} to T_{w1} without evaporation (occurring in the steam generator, T_{w1} generally coinciding with water saturation temperature) by cooling the coolant decreasing its temperature from T_{L1} to T_{L0}:

$$\dot{m}_L c_L (T_{L1} - T_{L0}) = \dot{m}_w c_w (T_{w1} - T_{w0}) = U_{LW} A_{LW} \frac{|(T_{L1} - T_{w1})(T_{L0} - T_{w0})|}{\left|ln\left(\frac{(T_{L1} - T_{w1})}{(T_{L0} - T_{w0})}\right)\right|} \quad (15)$$

$$\eta_{LW} = \frac{1 - e^{-(1-\omega_{LW})NTU_{LW}}}{1 - \omega_{LW} e^{-(1-\omega_{LW})NTU_{LW}}} \quad (16)$$

$$\omega_{LW} = \frac{min\left(\dot{m}_w c_w, \dot{m}_L c_L\right)}{max\left(\dot{m}_w c_w, \dot{m}_L c_L\right)} \quad (17)$$

$$NTU_{LW} = \frac{U_{LW} A_{LW}}{min\left(\dot{m}_w c_w, \dot{m}_L c_L\right)} \quad (18)$$

$$\dot{E}x_{LW} = -\dot{Q}_L\left(\frac{1}{T_w} - \frac{1}{T_L}\right) \quad (19)$$

Steam generator:

The last step is steam generation by mean of the exhausted gases. Enthalpy and exergy of exhausted gases are easily calculated using the same procedures as above:

$$h_{EG}(T_{EG0}, p_0) = h_{EG}(T_{EG1}, p_0) - \frac{\dot{m}_w[h_w(T_{w2}, p_w) - h_w(T_{w1}, p_w)]}{\dot{m}_{EG}} \quad (20)$$

$$\dot{E}x_{GW} = \dot{m}_{EG}(e_{EG1} - e_{EG0}) + \dot{m}_W(e_{W1} - e_{W2}) \quad (21)$$

As for the solution with microturbines, the schematic representation of the system is reported in Fig. 2, but the corresponding mass, energy and exergy balance equations are not shown, as they are very similar to those of Engine solution.

Photovoltaic power station:

With regard to photovoltaic producibility, reference was made to data from the PhotoVoltaic Geographic Information System (PVGIS) [45].

3. Dynamical simulation and optimal selection

For each configuration described above, in order to determine which are optimal, several simulations were performed by varying the power of both the CHP and the photovoltaic plant. The microturbines used in this paper had an electrical power of 100 kW or 200 kW in clusters up to 15. For the engine solutions, at most, two engines were used varying the power with a step of 50 kW for each one, up to a total power of 2 MWe. Finally, in order to properly design the solutions, appropriate operating maps of the machines involved were used. In any case, a single machine (ICE/MGT) is turned on and partialized only if a minimum electrical efficiency of 30% is guaranteed (Table 4).

Natural gas is the fuel used for the CHP. Entropy of vapors and gases are calculated using the thermodynamic properties stated in [43].

For the photovoltaic power plant, the maximum value of peak power for the whole plant was limited to 1 MWe (with 50 kW steps), taking into account the maximum surface area available in the company for the installation of the panels.

Lastly, if the CHP power supplied by the plant ($\dot{W}$) does not match the power required ($\dot{E}$), some electric energy is acquired from the National grid ($\dot{E} - \dot{W}$). This is taken into account by considering the average efficiency of the Italian energy generation system ($\eta = 0.46$) and so the global primary energy required by the entire farm.

A multi-objective optimization was performed to identify the best configuration and size of the system. The objective functions considered are:

- global (primary) energy efficiency $= \frac{\dot{E}}{\dot{m}_{CH_4} LHV + \frac{\dot{E} - \dot{W}}{\eta}}$

this represents the efficiency calculated by taking into account not only the CHP intrinsic efficiency (both heat and power $\dot{E}$ compared with energy provided by the fuel $\dot{m}_{CH_4} LHV$), but also that of the national grid (η).

- global exergy efficiency $= \frac{\sum \dot{E}x_i}{\dot{n}_m \varepsilon_{m,in}}$

this represents the overall exergy flux compared with that of the incoming components of air and fuel.

- Payback Period (PP) = Investment (I) / Cash Flow (CF)

as reported in [1], this is the most popular economic indicator and represents the period required to refund the initial capital plus the interest that could be received from an alternative investment of this capital.

Table 4
Electric efficiency of the ICEs and MGTs used in the simulation.

Partialization	ICE	MGT
100%	40.0	32.8
90%	38.0	32.8
75%	36.8	32.7
50%	35.2	30.7
25%	30.1	24.9

With regard to the choice of an optimal configuration from all the simulated ones, there are different possible algorithms that may be used [45-47]. In this case study, a Pareto (multi-objective) optimization technique was chosen. Pareto optimality allows establishing a hierarchy among the solutions of this multi-objective optimization problem [38].

The algorithm was developed in Matlab (The Mathworks inc., Natick – MA, USA). Fig. 3a,b show the operating logics of the developed software. These schemes were used for the calculation in each time interval, throughout the entire year. In particular, Fig. 3a specifies the logical steps that the algorithm performs to identify the optimal solutions in power tracking configuration. The evaluation is based on the assessment of the energy efficiency of the simulated solution. Therefore, it is necessary to verify whether the photovoltaic system alone is sufficient to cover the electrical load, or instead it is required to turn on the cogeneration units (at full or partial load). In order to optimize the solution, it is also considered the sale and purchase of energy from/to the grid. Indeed, it is worth remembering that the global energy efficiency also takes into account the efficiency of the national grid. In the case of heat tracking (Fig. 3b), the operating logics are structured in order to understand whether the configuration plant under investigation is able to cover the heating load or not, eventually by partializing some units or by activating a boiler or afterburner (ICEs or MGTs respectively) for the residual integration. Once the load is covered with an adequate efficiency, any deficit or surplus of electricity must be exchanged with the national grid.

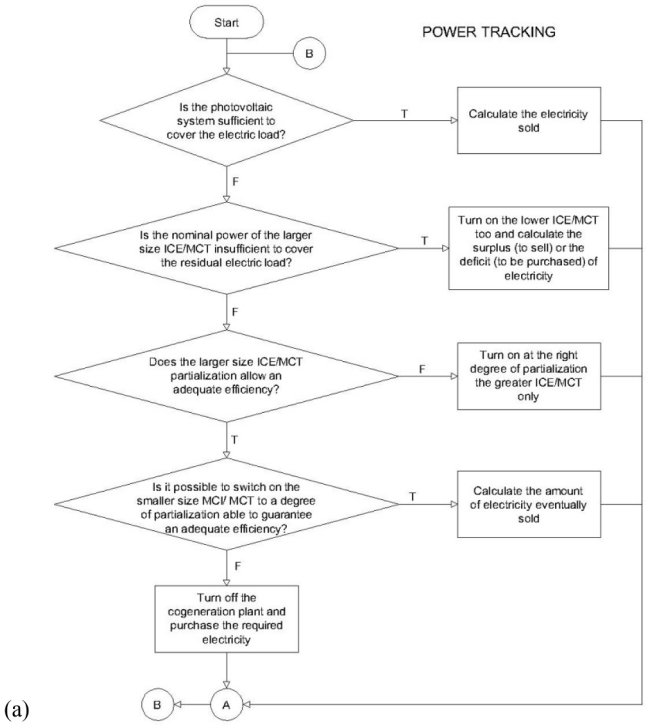

(a)

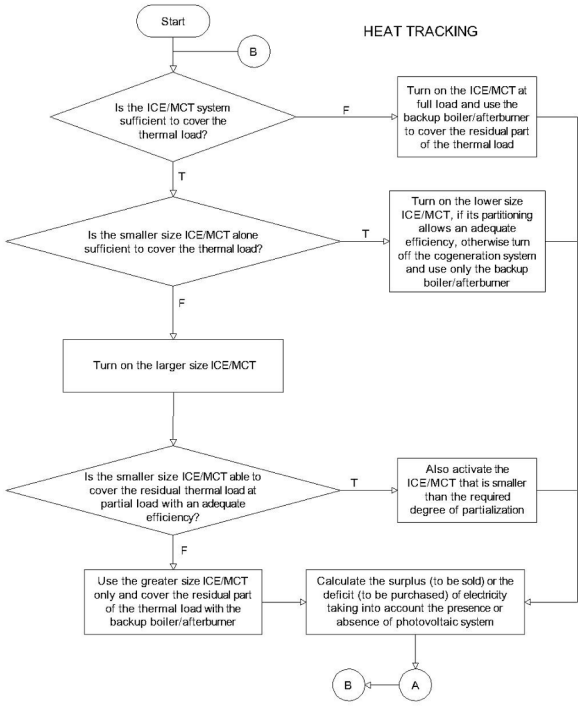

(b)

Fig. 3. Schematization of the operating logics for a) power tracking and b) heat tracking. The "A" operator stands for "calculation of process parameters", "B" represents "go back".

4. Results

4.1. Energetic analysis

Fig. 4 shows the monthly electricity and natural gas consumption of the boilers, converted into the corresponding amount of heat by considering that the LHV for natural gas is 9.6 kWh/Sm^3, from January to December. Fig. 4 also shows the monthly average heat/electric energy ratio (H/E). Although variable over the year, the monthly average H/E ratio remains above 1, with a yearly value average of 1.5. Therefore, according to conventional design rules [48-50], power tracking should be recommended as it seems that all cogenerated heat could be fully utilized. This analysis is, however, reductive, as it would lead to wrong dimensions.

By analyzing the cumulative curves of electricity and heat (Fig. 5a, b), it can be highlighted that an electrical load is always present, while a heat load is present only for at most 5,000 h. Therefore, the monthly average heat-power ratio seems to be greater than the yearly average value of 1.5 for no more than 5,000 h, and nearly zero (no heat required) for the remaining hours of the year. Therefore, according to this analysis, any CHP should be switched on for only 5,000 h per year and would cover only about 60% of the company's annual consumption. This consideration leads to two possible design choices:

1. downsizing the plant based on the monthly average data without taking the maximum advantage of the CHP (traditional method);
2. identifying other parameters that allow for the design of a system that tracks heat or power load as accurately as possible, trying to cover as much required energy as possible (proposed dynamical simulation).

The heat and power load trends from two different months, March and July (Fig. 6a,b), confirm the high variability of both electrical and heat load due to the seasonality of agricultural production as well as the lack of continuity in the supply of raw materials and demand for the finished products. In the summer months (May – September: e.g. Fig. 6b), the heat load is almost always higher than the power load due to the high demand for hot water for precooking and overheated steam for cooking. During the other months (January - April and October – December: e.g. Fig. 6a) there are long periods of an inversion of energy needs with the heat load often lower than the power load. This behavior is due to the smaller amount of raw materials to be processed during these periods with the resulting lower production of hot water and superheated steam.

It is also confirmed that there is a constant base of about 40% of the maximum electrical power required, essentially due to the continuous operation of cold storage for raw materials as well as for the finished

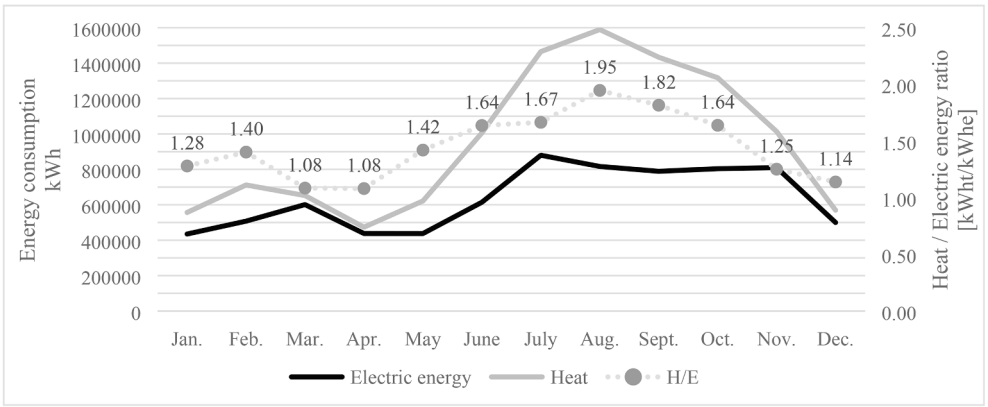

Fig. 4. Monthly energy consumption.

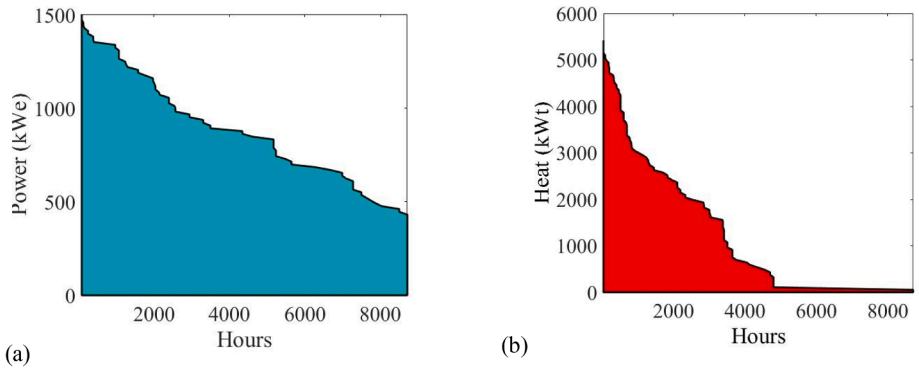

Fig. 5. Load duration curve: (a) power consumption; (b) heat consumption.

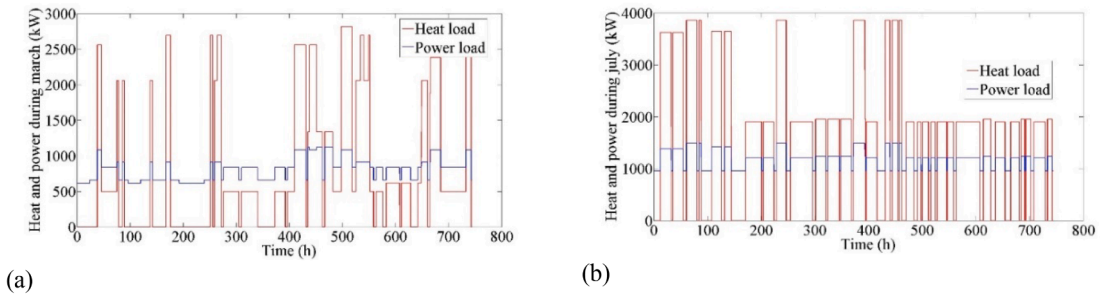

Fig. 6. Heat and power trend: (a) March; (b) July.

products.

Given the high demand for electric and thermal energy, it is also confirmed that the installation of a micro-grid composed of the cogeneration plant combined with photovoltaic panels could cover the basic electrical load during daytime.

4.2. Optimization results

The time trends of the results from dynamic simulation carried out using the numerical model described in the previous section were used to find the optimal plant configuration. Due to the very high number of plots, only those corresponding to the chosen solution and obtained by mean of a traditional design method are shown (see Section 4.3 below). On the other hand, all Pareto set plots are presented since they were used to determine the solutions from which to choose from the various simulated configurations. In particular, they are shown as two-dimensional diagrams for two pairs of parameters to be optimized, without loss of generality. In the diagrams for engine configurations, each point corresponds to a set of three values: the electric power of the first engine, the electric power of the second engine and the total electric power of the photovoltaic plant. In the case of the microturbines cluster, each point corresponds to a pair of values: the total electrical power of the microturbines and the total electrical power of the photovoltaic plant. The red dots represent the optimal configurations lying on the optimal Pareto boundary obtained through multi-objective analysis. For each set of configurations, the intersection of the different Pareto boundaries was found, thus obtaining the optimal solutions for each group of simulations, as shown below.

4.2.1. Internal combustion engines, photovoltaic, heat tracking

In this case, it is possible to choose a configuration which maximizes both energetic and exergetic objectives, 53.4% and 41.0% respectively (red dots to the far right in Fig. 7a,b) preserving an acceptable payback period (for about 3 years): first engine power 800 kWe, second engine

power 650 kWe and photovoltaic power 500 kWe. On the contrary, it is possible to achieve a shorter payback period (just more than 2 years, as shown in Fig. 7b) by reducing the energetic efficiency (near 45%), slightly reducing the installed power of the two ICEs. In this case, in fact, the CHP system does not cover the required power in most periods but leads to smaller investment costs. From the results highlighted in Fig. 7a, it is clear that the increase in energy efficiency is associated with an almost linear increase of the exergetic efficiency leading to a better use of the total energy in the studied industry.

4.2.2. Internal combustion engines, photovoltaic, power tracking

In the case of engine power tracking there are more possible solutions than previous cases that are characterized by a small reduction in the exergetic efficiency (just under 40%, Fig. 8a), a higher energy efficiency (more than 60%, Fig. 8b) and a lower payback period (less than 3 years).

In this case there are three possible configurations in the intersection of the two optimal sets. They are (First engine power, second engine power, Photovoltaic power): (850 kWe, 650 kWe, 550 kWe); (750 kWe, 750 kWe, 600 kWe); (700 kWe, 700 kWe, 600 kWe). The first configuration ensures the highest exergetic efficiency (38.2%). Otherwise, it is possible to slightly increase exergetic efficiency and drastically reduce the payback period at the expense of an important reduction in the global energetic efficiency. In fact, the first two solutions are characterized by the same power of the two ICEs, with quite similar efficiency both at full and partial loads.

4.2.3. Microturbines, photovoltaic and heat tracking

In this case (Fig. 9a,b), the best trade-off consists of 6 MGTs 200 kWe, 1 MGT 100 kWe and photovoltaic power 600 kWe. However, even with a quite high global-energy efficiency (68.7%) the payback period is quite high (3.8 years) and the exergy efficiency is quite low (30.0%).

This trend is principally due to the efficiency of the microturbines which drastically diminishes when the partialization falls below 50% (Table 4), determining the lowest quality of energy and thus a smaller exergetic efficiency. This is just the opposite compared to the behavior of the engines, which can be partialized with greater flexibility.

4.2.4. Microturbines, photovoltaic, power tracking

This last case is quite similar to the previous one, but the exergetic efficiency is lower than before (less than 30%, Fig. 10a). Payback period varies between 1.5 and 4 years (Fig. 10b): the higher the payback period the lower the quality of energy achieved. The configuration is similar to the previous one, but the photovoltaic installed power is 500 kWe.

In both of the microturbine cases it is possible to achieve very short payback periods at the expense of quite low exergetic efficiencies, leading to a possible higher environmental impact of these solutions than with the engines.

4.3. Dynamical VS static simulation: final results

Tables 5 and 6 show the best solutions (best trade-off with payback period of approximately 3 years) for each set of configurations obtained from the intersection of the Pareto boundaries described above. It is easy to observe that the cluster of MGTs allows higher overall energy efficiency (68.7%) than the use of the engines (53.4%) when choosing the heat tracking technique, while the global energetic efficiency is quite similar for power tracking for both the Engine and MGTs solutions. On the other hand, the exergetic efficiency is quite lower for MGTs, resulting in a poor use of the energy resources. In addition, a longer payback period is required if both energetic and exergetic objectives are maximized in all cases.

Focusing on tracking methods for the engine solution, even if power tracking allows a CHP-only efficiency that is lower than heat tracking, the overall efficiency is significantly higher, while the two methods are almost equivalent as regards both global exergetic efficiency and payback period. Hence, power tracking is chosen.

On the contrary, in the case of a solution with MGTs, while again there is a little difference in both exergetic global efficiency and payback period between the two tracking methods, heat tracking is the best method regarding both global and CHP energetic efficiency.

Moreover, while the cluster of MGTs allows for higher overall energy efficiency than the use of the engines for both tracking methods, a longer payback period is required and the exergetic efficiency is moderately lower, resulting in higher operating costs and a poorer use of the energy resources.

Therefore, in the present study engine technology with power tracking represents the best choice, mainly because of the high variability of power and heat load. The configuration to be installed is the one that includes two engines with power equal to 650 kWe and 850 kWe respectively and a photovoltaic plant of peak power equal to 550 kWe (Fig. 11). On the contrary, when a quite high simultaneity between electric and heat load occurs, the employment of microturbine technology becomes cheaper than the engines, as in the case of the pasta factory reported in [51].

In Fig. 12 and 13, an example of the required electric power trends in a cold and hot month (as already shown in Fig. 6) are compared with those produced in the chosen cogeneration plant solution. Thus, higher generated electric power than required means that some electrical energy is sold, while smaller values lead to acquire it. Heat is always slightly smaller than required and the heat deficit is generated using the backup boiler. During the year, the surplus/deficit of generated electrical energy does not exceed 4% of the total energy required.

The ICE configuration with power tracking, obtained by means of dynamical simulation, is compared to the configuration obtained using the classical static technique. In this case, (the electric power required is just below 2 MW and the average heat/power ratio is about 1.5), a CHP

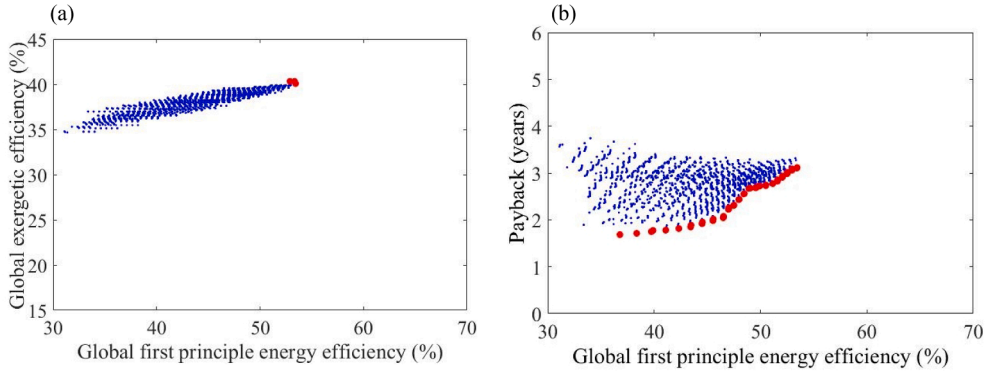

Fig. 7. (a) Pareto Set (red dots) for the pair of criteria: Global (primary) exergetic efficiency - Global (primary) energy efficiency**;** (b) Pareto Set (red dots) for the pair of criteria: Payback – Global (primary) energy efficiency. (For interpretation of the references to colour in this figure legend, the reader is referred to the web version of this article.)

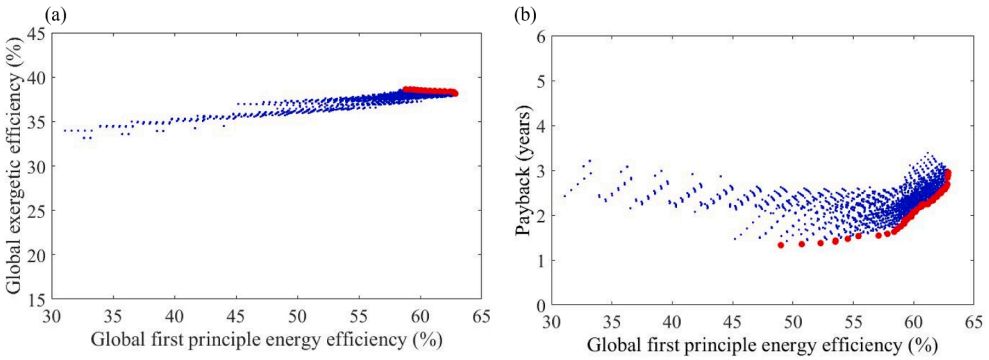

Fig. 8. (a) Pareto Set (red dots) for the pair of criteria: Global (primary) exergetic efficiency - Global (primary) energy efficiency. (b) Pareto Set (red dots) for the pair of criteria: Payback - Global (primary) energy efficiency. (For interpretation of the references to colour in this figure legend, the reader is referred to the web version of this article.)

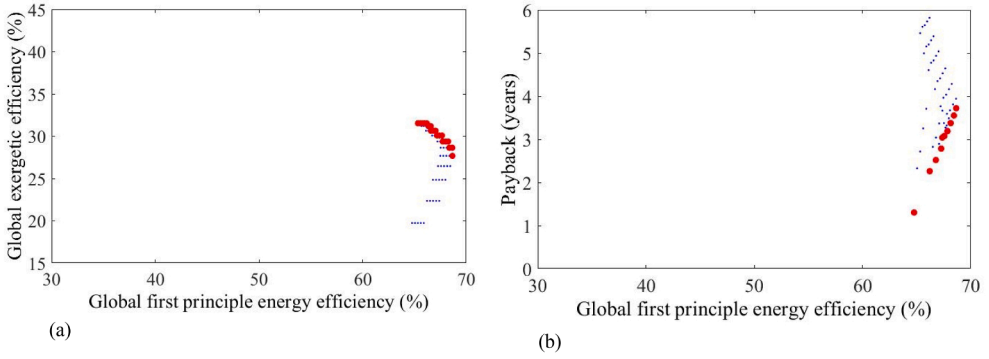

Fig. 9. (a) Pareto Set (red dots) for the pair of criteria: Global (primary) exergetic efficiency - Global (primary) energy efficiency. (b) Pareto Set (red dots) for the pair of criteria: Payback - Global (primary) energy efficiency. (For interpretation of the references to colour in this figure legend, the reader is referred to the web version of this article.)

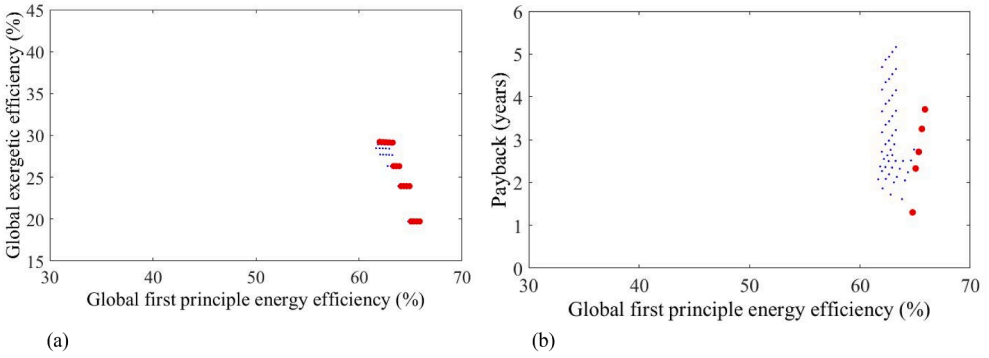

Fig. 10. (a) Pareto Set (red dots) for the pair of criteria: Global (primary) exergetic efficiency - Global (primary) energy efficiency; (b) Pareto Set (red dots) for the pair of criteria: Payback - Global (primary) energy efficiency. (For interpretation of the references to colour in this figure legend, the reader is referred to the web version of this article.)

Table 5
Optimal solutions for engine configurations.

Parameter	Heat Traking	Power tracking
First engine power (kWe)	800	850
Second engine power (kWe)	500	650
Photovoltaic power (kWe)	550	550
Payback (years)	3.1	2.9
Global (primary) energetic efficiency (%)	53.4	62.8
Plant (CHP only) energetic efficiency (%)	70.0	60.0
Global exergetic efficiency (%)	41.0	38.2

Table 6
Optimal solutions for microturbines configurations.

Parameter	Heat Traking	Power tracking
Microturbines power (kWe) (6 MGTs 200 kWe and 1 MGT 100 kWe)	1300	1300
Photovoltaic power (kWe)	600	500
Payback (years)	3.8	3.7
Global (primary) energetic efficiency (%)	68.7	63.4
Plant (CHP only) energetic efficiency (%)	73.2	65.3
Global exergetic efficiency (%)	30.0	29.0

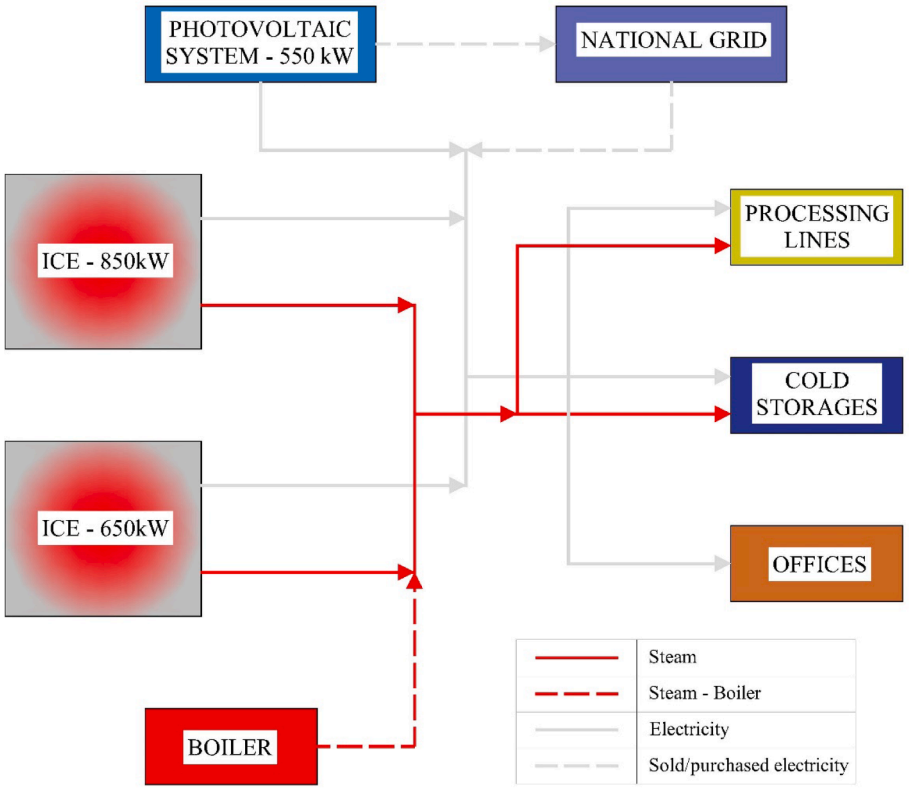

Fig. 11. Schematic representation of the best configuration of the CHP plant (power tracking).

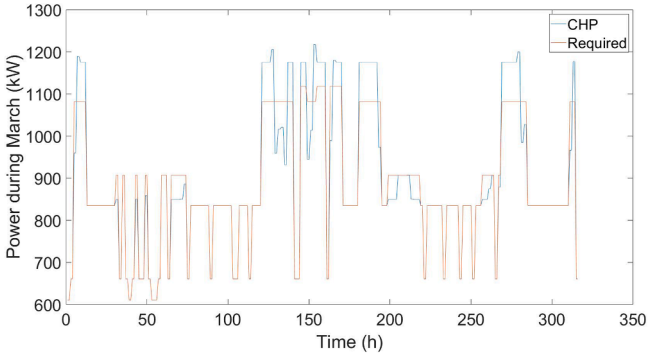

Fig. 12. Electric power trend in March: 'CHP' line corresponds to the power generated by the cogeneration plant configuration obtained by dynamic simulation; 'Required' corresponds to the electric power absorbed by the whole firm (see also Fig. 6a).

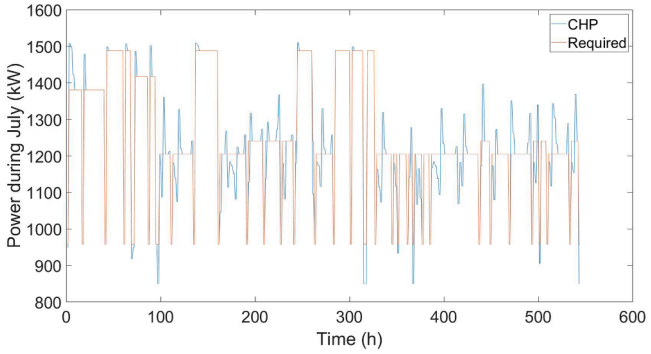

Fig. 13. Electric power trend in July: 'CHP' line corresponds to the power generated by the cogeneration plant obtained by dynamic simulation; 'Required' corresponds to the electric power absorbed by the whole firm (see also Fig. 6b).

plant usually consists of two engines of equal power (450 kWe each). This overall power is calculated based on the average power required by the company in the reference year taken from energy bills: average monthly consumption, installed power and a typical load curve (in this case, based on the annual load curves of Fig. 5a, b).

Since there is a basic demand of electrical energy regardless of the heat load (cold stores) equal to approximately 530 kWe, it is generally recommended to install a photovoltaic plant of 550 kWp. Table 7 shows the results from simulations carried out by following the above criteria of classical design.

Power tracking is the best choice in this case as well. Then Table 8 compares the best solutions for both dynamical and static design. In particular, it is noted that the overall electrical power determined with the dynamic design is greater than that obtained with a traditional static design method. This means that the classical design produces an underestimation of the real demand for electric energy, with the reduction of the overall efficiency of the overall electrical grid system.

In Figs. 14 and 15, the required electric power trends (giving examples of a cold and hot month) are compared with those produced with the CHP configuration obtained by static procedure. It is clear that in both months (with similar behavior during the year) the electric power generated by the CHP designed using the traditional (static) procedure almost never covers the amount required with a deficit greater than 20%.

The difference in energy and exergetic efficiencies is in favor of the design based on a dynamic simulation, and the payback is less than three years in both cases. A further analysis has been carried out by using one more objective function: the annual savings of the proposed solution (based on annual energy costs of the company). The results (data not shown) highlight that the global annual savings is 12% higher for the

Table 7
System-related outputs designed according to the classical design method based on the average data.

Parameter	Heat Traking	Power tracking
First engine power (kWe)	450	450
Second engine power (kWe)	450	450
Photovoltaic power (kWe)	550	550
Payback (years)	3.2	2.5
Global (primary) energetic efficiency (%)	47.0	56.6
Plant (CHP only) energetic efficiency (%)	70.4	36.9
Global exergetic efficiency (%)	38.0	36.9

Table 8
Dynamic and static design for a cogeneration plant consisting of two internal combustion engines with electrical load tracking.

Parameter	Dynamic design	Static design
First engine power (kWe)	650	450
Second engine power (kWe)	850	450
Photovoltaic power (kWe)	550	550
Payback (years)	2.9	2.5
Global (primary) energetic efficiency (%)	62.8	56.6
Plant (CHP only) energetic efficiency (%)	60.0	58.6
Global exergetic efficiency	38.2	36.9

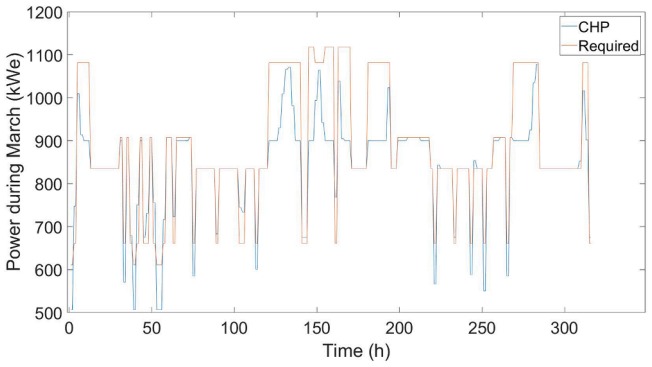

Fig. 14. Electric power trend in March: 'CHP' line corresponds to the generated power by the CHP plant obtained by static design, 'Required' corresponds to the electric power absorbed by the whole firm (see also Fig. 6a).

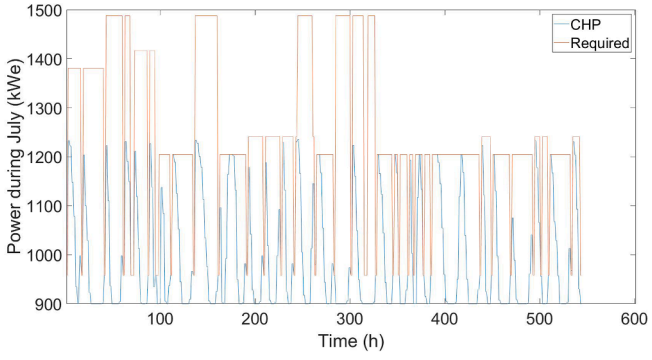

Fig. 15. Electric power trend in July: 'CHP' line corresponds to the generated power by the CHP plant obtained by static design n, 'Required' corresponds to the electric power absorbed by the whole firm (see also Fig. 6b).

dynamically designed solution than that obtained with the traditional design technique. This allows, when compared with a greater absolute cost of the cogeneration plant (hence a slightly higher payback), more annual investment margins in favor of the company.

From the point of view of CHP alone, it seems that the two solutions do not show great difference in terms of energy efficiency and, therefore, it seems that a more accurate design leads to only economic benefits. This analysis, however, was completed by taking into account the global energy efficiency of the CHP that includes also the National grid system efficiency. This overall efficiency is 6% higher in the case of dynamic design, determining better overall use of resources and less environmental impact.

Therefore, the results obtained confirm the validity of the proposed method both in terms of energy savings and exergetic benefits as well as a reduced environmental impact.

5. Conclusions

The aim of this paper is to propose a method for designing and dimensioning a cogeneration plant for a food processing factory by using dynamic simulation and multi-objective optimization analysis. The proposed procedure first of all requires that the designer has to acquire one year real data about the use of energy in the studied industry and use these data as input to the simulation model. The solution found through dynamic analysis should be compared to that obtained with a standard design method (static analysis) as done in this paper. Therefore, the proposed technique can be used effectively when there is a high variability of the electrical and / or heat load. In the studied application, the high demand and variability of both electrical and heat load led to consider two configurations of cogeneration system: 1) with pressurized internal combustion engines and a backup boiler; 2) with gas microturbines plus afterburner. The results gives as optimal solution an energy generation plant equipped with two engines of 650 kW and 850 kW respectively and a 550 kW photovoltaic plant. Globally, what obtained by the dynamical simulation can be summarized as follows:

- the proposed method allows the choice of the most suitable technology, among those proposed, in order to fit the factory energy demand and determine the correct size of the cogeneration units;
- the overall efficiency is 6% higher with dynamic rather than with static design by considering the cogeneration system + national grid;
- the surplus/deficit of generated electrical energy does not exceed 4% of the total required energy;
- the traditional (static) procedure almost never covers the amount required with the resulting deficit greater than 20%;
- the annual savings resulting from the solution found through dynamic analysis is 12% higher than that obtained by mean of the standard method.

The results prove that dimensioning cogeneration systems through dynamic analysis and multi-objective optimization can lead to high profitability in terms of both energetic benefits and environmental impact. For a future perspective, the method could be further enhanced to optimize the monitoring of the CHP plant during operations, after its optimal selection.

CRediT authorship contribution statement

Filippo Catalano: Conceptualization, Methodology, Software, Writing - original draft. **Claudio Perone:** Formal analysis, Data curation, Investigation, Writing - original draft. **Valentino Iannacci:** Writing - original draft, Validation. **Alessandro Leone:** Validation. **Antonia Tamborrino:** Investigation. **Biagio Bianchi:** Supervision.

Declaration of Competing Interest

The authors declare that they have no known competing financial interests or personal relationships that could have appeared to influence the work reported in this paper.

Acknowledgments

This paper is dedicated to the memory of Professor Bernardo Fortunato (Polytechnic of Bari). During his academic career, Professor Bernardo Fortunato developed research activities based on Energy Integrated System and he has contributed to the first conceptualization of the present research.

References

[1] Bianco V, De Rosa M, Scarpa F, Tagliafico LA. Implementation of a cogeneration plant for a food processing facility. A case study. Appl Therm Eng 2016;102:500–12.
[2] Isa NM, Tan CW, Yatim AHM. A comprehensive review of cogeneration system in a microgrid: A perspective from architecture and operating system. Renew Sustain Energy Rev 2018;81:2236–63.
[3] Chand MRR, Ibrahim H, Azran Z, Arshad A, Basrawi F, Che Ghani SA, Alias A, Mamat R, Rahman MM. Review on Recent Development Micro Gas Turbine -Trigeneration System and Photovoltaic Based Hybrid Energy System. MATEC Web Conf. 2016;74:00028. https://doi.org/10.1051/matecconf/20167400028.
[4] Al Moussawi H, Fardoun F, Louahlia-Gualous H. Review of tri-generation technologies: Design evaluation, optimization, decision-making, and selection approach. Energy Convers Manage 2016;120:157–96.
[5] Ibrahim TK, Mohammed MK, Awad OI, Abdalla AN, Basrawi F, Mohammed MN, Najafi G, Mamat R. A comprehensive review on the exergy analysis of combined cycle power plants. Renew Sustain Energy Rev 2018;90:835–50.
[6] Kasaeian A, Nouri G, Ranjbaran P, Wen D. Solar collectors and photovoltaics as combined heat and power systems: A critical review. Energy Convers Manage 2018;156:688–705.
[7] Chai DS, Wen JZ, Nathwani J. Simulation of cogeneration within the concept of smart energy networks. Energy Convers Manage 2013;75:453–65.
[8] Wang Y, Shi Y, Luo Yu, Cai N, Wang Y. Dynamic analysis of a micro CHP system based on flame fuel cells. Energy Convers Manage 2018;163:268–77.
[9] Dorer V, Weber A. Energy and CO2 emissions performance assessment of residential micro-cogeneration systems with dynamic whole-building simulation programs. Energy Convers Manage 2009;50(3):648–57.
[10] Marrasso E, Roselli C, Sasso M, Picallo-Perez A, Sala Lizarraga JM. Dynamic simulation of a microcogeneration system in a Spanish cold climate. Energy Convers Manage 2018;165:206–18.
[11] Nejat P, Jomehzadeh F, Taheri MM, Gohari M, Abd. Majid MZ. A global review of energy consumption, CO 2 emissions and policy in the residential sector (with an overview of the top ten CO 2 emitting countries). Renew Sustain Energy Rev 2015;43:843–62.
[12] Chowdhury JI, Hu Y, Haltas I, Balta-Ozkan N, Matthew GJ, Varga L. Reducing industrial energy demand in the UK: A review of energy efficiency technologies and energy saving potential in selected sectors. Renew Sustain Energy Rev 2018;94:1153–78.
[13] Manan ZA, Mohd Nawi WNR, Wan Alwi SR, Klemeš JJ. Advances in process integration research for CO2 emission reduction – A review. J Cleaner Prod 2018;167:1–13. https://doi.org/10.1016/j.jclepro.2017.08.138.
[14] Delpech B, Axcell B, Jouhara H, Kaźmierczak B, Kutyłowska M, Piekarska K, Jouhara H, Danielewicz J. A review on waste heat recovery from exhaust in the ceramics industry. E3S Web Conf. 2017;22:00034. https://doi.org/10.1051/e3sconf/20172200034.
[15] Oliveira T, Varum C, Botelho A. Econometric modeling of CO2 emissions abatement: Comparing alternative approaches. Renew Sustain Energy Rev 2019;105:310–22.
[16] Tamborrino A, Perone C, Catalano F, Squeo G, Caponio F, Bianchi B. Modelling Energy Consumption and Energy-Saving in High-Quality Olive Oil Decanter Centrifuge: Numerical Study and Experimental Validation". Energies 2019;12:2592.
[17] Leone A, Romaniello R, Zagaria R, Sabella E, De Bellis L, Tamborrino A. Machining effects of different mechanical crushers on pit particle size and oil drop distribution in olive paste: Crushing vs. pits particle size and oil drops distribution. Eur. J. Lipid Sci. Technol. 2015;117(8):1271–9.
[18] Leone A, Tamborrino A, Zagaria R, Sabella E, Romaniello R. Plant innovation in the olive oil extraction process: A comparison of efficiency and energy consumption between microwave treatment and traditional malaxation of olive pastes. J Food Eng 2015;146:44–52.
[19] Leone A, Romaniello R, Peri G, Tamborrino A. Development of a new model of olives de-stoner machine: Evaluation of electric consumption and kernel characterization. Biomass Bioenergy 2015;81:108–16.
[20] Philipp M, Schumm GM, Peesel R-H, Walmsley TG, Atkins MJ, Hesselbach J. Optimal energy supply structures for industrial sites in different countries considering energy transitions: A cheese factory case study. Chem Eng Trans 2016;52:175–80. https://doi.org/10.3303/CET1652030.
[21] Bianco, V., De Rosa, M., Scarpa, F., Tagliafico, L.A., Feasibility study of a cogeneration plant: the case of a processing facility of the beverage sector, ASME-ATI-UIT 2015 Conference on Thermal Energy Systems: Production, Storage, Utilization and the Environment, 17 – 20 May, 2015, Napoli, Italy.
[22] Winfried R, Roland M-P, Alexander D, Jürgen L-K. Usability of food industry waste oils as fuel for diesel engines. J Environ Manage 2008;86(3):427–34.
[23] International Energy Agency, Cogeneration and Renewables - Solutions for low-carbon energy future, OECD/IEA, 2011, Paris: http://www.cogeneurope.eu/medialibrary/2011/05/18/9c8a6f7e/110511%20IEA%20report%20-%20Cogeneration%20and%20renewables.pdf.
[24] Fantozzi F, Ferico SD, Desideri U. Study of a cogeneration plant for agro-food industry. Appl Therm Eng 2000;20(11):993–1017.
[25] Freschi F, Giaccone L, Lazzeroni P, Repetto M. Economic and environmental analysis of a trigeneration system for food-industry: A case study. Appl Energy 2013;107:157–72.
[26] Aghbashlo M, Mobli H, Rafiee S, Madadlou A. A review on exergy analysis of drying processes and systems. Renew Sustain Energy Rev 2013;22:1–22.
[27] Zheng CY, Wu JY, Zhai XQ, Yang G, Wang RZ. Experimental and modeling investigation of an ICE (internal combustion engine) based micro-cogeneration device considering overheat protection controls. Energy 2016;101:447–61.
[28] Acevedo, L., Uche J., Del Almo, A., Círez F., Usón S., Martínez A. and Guedea I. Dynamic Simulation of a Trigeneration Scheme for Domestic Purposes Based on Hybrid Techniques. Energies, 2016, 9, 1013-1037.
[29] Campos-Celador Á, Pérez-Iribarren E, Sala JM, del Portillo-Valdés LA. Thermoeconomic analysis of a micro-CHP installation in a tertiary sector building through dynamic simulation. Energy 2012;45(1):228–36.
[30] PANNO D, MESSINEO A, DISPENZA A. Cogeneration plant in a pasta factory: Energy saving and environmental benefit. Energy 2007;32(5):746–54.
[31] Ciampi G, Rosato A, Scorpio M, Sibilio S. Energy, Environmental and Economic Dynamic Simulation of a Micro-Cogeneration System Serving an Italian Multi-Family House. Energy Procedia 2015;78:1141–6.
[32] Calise F., Capuano D., Vanoli, L. Dynamic Simulation and Exergo-Economic Optimization of a Hybrid Solar–Geothermal Cogeneration Plant. Energies, 2015, 8, 2606-2646.
[33] Ahmadi P, Almasi A, Shahriyari M, Dincer I. Multi-objective optimization of a combined heat and power (CHP) system for heating purpose in a paper mill using evolutionary algorithm. Int. J. Energy Res. 2012;36(1):46–63.
[34] Zisopoulos FK, Rossier-Miranda FJ, van der Goot AJ, Boom RM. The use of exergetic indicators in the food industry – A review. Crit Rev Food Sci Nutr 2017;57(1):197–211.
[35] Fu C, Gundersen T. Using exergy analysis to reduce power consumption in air separation units for oxy-combustion processes. Energy 2012;44(1):60–8.
[36] Gimelli A, Muccillo M. Optimization criteria for cogeneration systems: Multy-objective approach and application in an hospital facility. Appl Energy 2013;104:910–23.
[37] Piacentino A, Cardona F. An original multi-objective criterion for the design of small-scale polygeneration systems based on realistic operating conditions. Appl Therm Eng 2008;28(17-18):2391–404.
[38] Toffolo A, Lazzaretto A. Evolutionary algorithms for multi-objective energetic and economic optimization in thermal system design. Energy 2002;27:549–67.
[39] Buonomano A, De Luca G, Figaj RD, Vanoli L. Dynamic simulation and thermo-economic analysis of a PhotoVoltaic/Thermal collector heating system for an indoor–outdoor swimming pool. Energy Convers Manage 2015;99:176–92.
[40] McBride B. J, Zehe M.J., Gordon S. NASA Glenn Coefficients for Calculating Thermodynamic Properties of Individual Species. NASA Technical Paper 2002-211556, NASA Glenn Research Center, Cleveland, OH.
[41] Wang J, Youa S, Zong Yi, Træholt C. Zhao Yang Dong, You Zhou. Flexibility of combined heat and power plants: A review of technologies and operation strategies. Appl Energy 2019;252:113445.
[42] ENERGY SAVER Cogeneration feasibility guide, Office of Environment and Heritage, Government of New South Wales, Australia, 2000, pag. 26. https://www.environment.nsw.gov.au/resources/business/140685-cogeneration-feasibility-guide.pdf.
[43] Bianchi, B., Cavone, G., Cice, G., Tamborrino, A., Amodio, M., Capotorto, I., & Catalano, P. CO2 employment as refrigerant fluid with a low environmental impact. experimental tests on arugula and design criteria for a test bench. Sustainability, 2015, 7(4), 3734-3752.
[44] Ghannadzadeh A, Thery-Hetreux R, Baudouin O, Baudet P, Floquet P, Joulia X. General methodology for exergy balance in ProSimPlus® process simulator. Energy 2012;44(1):38–59.
[45] Photovoltaic Geographical Information System (PVGIS), http://re.jrc.ec.europa.eu/pvg_tools/en/tools.html.
[46] Arcuri P, Florio G, Fragiacomo P. A mixed integer programming model for optimal design of trigeneration in a hospital complex. Energy 2007;32(8):1430–47.
[47] Khani L, Mehr AS, Yari M, Mahmoudi SMS. Multi-objective optimization of an indirectly integrated solid oxide fuel cell-gas turbine cogeneration system. Int J Hydrogen Energy 2016;41(46):21470–88.
[48] Cai Bo, Li H, Hu Y, Zhang G. Operation strategy and suitability analysis of CHP system with heat recovery. Energy Build 2017;141:284–94.

[49] Gu Q, Ren H, Gao W, Ren J. Integrated assessment of combined cooling heating and power systems under different design and management options for residential buildings in Shanghai. Energy Build 2012;51:143–52.
[50] Smith AD, Mago PJ. Effects of load-following operational methods on combined heat and power system efficiency. Appl Energy 2014;115:337–51.
[51] Perone C, Catalano F, Giametta F, Tamborrino A, Bianchi B, Ayr U. Study and analysis of a cogeneration system with microturbines in a food farming of dry pasta. Chem Eng Trans 2017;58:499–504.